CELL CYCLE
2021, VOL. 20, NO. 1, 126–141
https://doi.org/10.1080/15384101.2020.1864128

Taylor & Francis
Taylor & Francis Group

RESEARCH PAPER

lncRNA ZFAS1 contributes to the radioresistance of nasopharyngeal carcinoma cells by sponging hsa-miR-7-5p to upregulate ENO2

Jiaojiao Peng, Feng Liu, Hong Zheng, Qi Wu, and Shixi Liu

Department of Otolaryngology, Head and Neck Surgery, West China Hospital, Sichuan University, Sichuan, China

ABSTRACT

Previous research revealed that lncRNA ZFAS1 could promote nasopharyngeal carcinoma (NPC) by inhibiting its downstream target axis. However, the association between ZFAS1 and radioresistant NPC cells is unclear. This study aimed to explore the roles of ZFAS1 in the radioresistance of NPC. Bioinformatics analysis was conducted to identify the significant factors (ENO2 and miR-7-5p) that contributed to the radioresistance of NPC cells. After performing qRT-PCR analysis, we found that the expression of ZFAS1 and ENO2 was upregulated in NPC cells but that the miR-7-5p expression was downregulated in the same samples. Apart from that, we noticed that ZFAS1 inhibition enhanced the sensitivity of NPC cells to radiation therapy by repressing cell proliferation and promoting cell apoptosis. Subsequently, we found that ZFAS1 could sponge miR-7-5p to upregulate ENO2, which was the target of miR-7-5p. Experimental results also indicated that the suppression of miR-7-5p inhibited the sensitivity of NPC cells to radiation therapy, thereby suppressing ENO2 expression. Overall, our findings suggested that ZFAS1 contributed to the radioresistance of NPC cells by regulating the miR-7-5p/ENO2 axis and that ZFAS1 might be a potential therapeutic target for addressing the radioresistance of NPC cells.

ARTICLE HISTORY
Received 15 April 2020
Revised 7 November 2020
Accepted 11 December 2020

KEYWORDS
LncRNA; tumor suppressor; glycolysis (Warburg effect); HIF1-alpha; nasopharyngeal carcinoma and tumor resistance

Introduction

Nasopharyngeal carcinoma (NPC) can be described as a type of malignant tumors found around the end of the nose and the back of the throat. Even though this malignancy is rare around the globe, the morbidity and mortality rate in China is relatively high compared to other nations [1]. The prognosis of patients with NPC is usually poor due to its early distant metastasis [2,3]. Epstein-Barr virus is often considered as a risk factor in the development of NPC, and other important risk factors of NPC include smoking, eating nitrosamine dietary, long-term exposure to chemical carcinogens, and genetic susceptibility [4,5]. Today, radiotherapy is the main treatment for patients with NPC [6,7]. Nonetheless, the prognosis of NPC is still poor for a number of patients with radioresistant cells [7,8]. Therefore, it crucial to discover how to reverse the radioresistance of NPC patients.

Long noncoding RNAs (lncRNAs) refer to RNA molecules with more than 200 nucleotides in length and with the ability to regulate gene expression at multiple levels [9]. Recent studies have shown that lncRNAs are involved in many crucial regulatory processes, including X-chromosome silencing, genomic imprinting, chromatin modification, transcriptional activation, and transcriptional interference [10–14]. Located at the chromosome 20q13.13 with the exon count of 5, lncRNA ZFAS1 was first discovered in breast cancer [15]. Some studies reported that the expression of ZFAS1 contributed to the metastasis of hepatocellular carcinoma, prostate cancer, colorectal cancer and esophageal squamous cell carcinoma [16–19]. In our previous study, we found that lncRNA ZFAS1 promoted the growth of samples with NPC [20]. However, we are yet to demonstrate whether ZFAS1 could influence the radioresistance of NPC cells.

MiRNAs have been found to play an essential role in the growth of many cancers, including pancreatic cancer, breast cancer, prostate cancer, colorectal cancer, gastric cancer, lung squamous cell carcinoma, and ovarian cancer [21–27]. The involvement of miR-7-5p in human cancer has been fully investigated in the last six years. However, the participation

CONTACT Shixi Liu cdliushixi@163.com
Supplemental data for this article can be accessed here.

of miR-7-5p in the radioresistance of NPC has never been studied. In 2019, a team of researchers documented that miR-7-5p was upregulated in clinically resistant cell lines HeLa (cervical cancer cell lines) and SAS cell lines (oral squamous cell carcinoma) [28]. In addition, the controversial roles of miR-7-5p in chemo-drug resistance have been reported in human hepatocellular carcinoma [29], cervical cancer [30], breast cancer [31], and small cell lung cancer [32]. Nonetheless, scientists are yet to unravel whether miR-7-5p could enhance the radioresistance of NPC tissues.

ENO2 can be referred to as an enzyme found in mammals [33]. ENO2 was majorly located in mature neurons and was found to be highly expressed in such cancers as glioblastoma, neuroendocrine prostate cancer, and renal cell carcinoma [34–36]. The development of cancer was also discovered to be associated with the development of dynamic metabolic patterns [37,38]. During the occurrence and development of tumors, the main metabolism pattern of tumor cells is glycolysis [39]. This metabolism pattern helps in accelerating the proliferation of tumor cells and developing tumors [40]. A study showed that the level of glycolysis metabolism gradually increased during the development of liver cancer [41]. Another research documented that glycolytic inhibitors, in conjunction with chemotherapy, could improve hepatocellular carcinoma treatments [42]. We performed a bioinformatics analysis and found that ENO2 was associated with glycolytic and the HIF pathways in radioresistant NPC cells. Evidence in the literature review also confirmed that the expression of ENO2 could induce the expression of glycolysis-related genes and promote glycolysis progression, thereby enhancing the resistance of leukemia cells to chemotherapy [43]. Furthermore, a report suggested that ENO2 was a responsive gene of HIF, which participated in the development of tumor growth [44]. In short, we identified ENO2 to be a potential downstream effector of miR-7-5p and predicted that this isoenzyme might be involved in the radioresistance of NPC cells.

We aimed in this paper to explore the roles of ZFAS1 in the radioresistance of NPC cells. We hypothesized that IncRNA ZFAS1 could contribute to the radioresistance of NPC cells by sponging hsa-miR-7-5p to upregulate ENO2. We also predicted that ZFAS1 might be a potential therapeutic target for addressing the radioresistance of NPC cells. Our research is relevant in that it could provide better and effective long-term NPC treatments for patients with radioresistant cells.

Materials and methods

Tissues collection

Fifty-five patients who were diagnosed with NPC in West China Hospital, Sichuan University participated in this study. This research was approved by the Ethics Committee of West China Hospital, Sichuan University. NPC tissues and adjacent healthy tissues were frozen before the experiments were performed and before clinical characteristics were recorded. The collection procedure and the use of tissues were done according to the ethical standards developed by the Helsinki Declaration. The clinical characteristics of the participants are summarized in Supplementary Table 1.

Cell culture

Cell lines were bought from BeNa Culture Collection (China), such as human NPC cell lines (SUNE-1, 5–8 F, HNE-3and C666-1 cell lines) and non-tumoral nasal mucosal epithelial cell line NP-69. SUNE-1, 5–8 F, HNE-3and C666-1 cell lines were cultured in RPMI-1640 media supplemented with 10% FBS (fetal bovine serum).

RNA was detected by real-time quantification PCR

The total RNA was first isolated using TRIzol reagents (DP501, Tiangen Biochemical, China). After checking the purity of RNA, the RNA was reverse-transcribed into cDNA using a cDNA synthesis kit (KR211, Tiangen Biochemical, China). Next, the expression of lncRNA ZFAS1, miR-7-5p and ENO2 mRNA was analyzed using the SYBR Green PCR Kit (FP411, Tiangen Biochemical, China). U6 acted as a reference gene for miR-7-5p, while

GAPDH served as a reference gene for lncRNA ZFAS1 and ENO2 mRNA. The primer sequences are displayed in Supplementary Table 2.

Cell fractionation

The Invitrogen PARIS Kit (ThermoFisher, AM1921, USA) was utilized to separate and purify cytoplasmic and nuclear RNAs. This process was done according to the instructions of the manufacturer. Also, the expression levels of lncRNA ZFAS1, GAPDH (cytoplasmic control) and U6 (nuclear control) were examined using qRT-PCR.

Cell transfection

Si-ZFAS1-1, si-ZFAS1-2, miR-7-5p inhibitor, ENO2 siRNA (si-ENO2), and si-NC were designed and synthesized by Tiangen Biochemical (Beijing, China). After the confluence of cells reached 60%, the Lipofectamine 2000 Transfection Reagent (ThermoFisher, 11668027, USA) was used to transfect the plasmids into target cells (SUNE-1 and C666-1 cell lines).

Luciferase reporter assay

Constructed plasmids containing wild type or mutant type of lncRNA ZFAS1 and ENO2 mRNA were purchased from Tiangen Biochemical (Beijing, China). These plasmids were then transfected into SUNE-1 and C666-1 cell lines (60% confluence) using the Lipofectamine 2000 Transfection Reagent (ThermoFisher, 11668027, USA). Next, miR-892b mimics were co-transfected into the cells with the same method. After 48 hours, the cells were gathered and lysed with lysis buffer. The dual-luciferase reporter assay system (GeneCopoeia, LF031, China) was also used to analyze the relative luciferase activity.

RNA pull-down assay

This experiment was performed using Magnetic RNA-Protein Pull-Down Kit (ThermoFisher, 20164, USA) according to the manufacturer's instruction. First, miR-7-5p, antisense oligo, and miR-7-5p mutant were labeled with biotin, which could bind to the streptavidin magnetic beads. The lysates of SUNE-1 and C666-1 cell lines were then incubated with biotin-labeled miR-7-5p, antisense oligo, and miR-7-5p mutant. It was observed that only biotin-labeled miR-7-5p could bind to the target in a RISC dependent manner. Then, the incubated lysate samples were allowed to pass through the streptavidin magnetic beads. The elusion was done using the non-denaturing Biotin Elution Buffer or SDS-PAGE Loading Buffer. Finally, qRT-PCR analysis was performed to measure the expression of lncRNA ZFAS1 or miR-7-5p in the elution.

CCK-8 assay

Cell Counting Kit-8 (CCK-8) was purchased from Dojindo Laboratories (Kumamoto, Japan) to determine the cell viability of NPC cells. The 3×10^3 cells/well cells were seeded in 96-well plates overnight. Next, the cell viability of the samples was detected within a certain range of radiation doses (0, 4, and 8 Gy). After that, the cell viability of each group was detected at four different periods (24, 48, 72 and 96 h). 10 μL CCK-8 solution was added to every well before the cells were incubated for 2 h. The absorbance of the cells in every well was eventually read at 450 nm using an ELISA plate reader.

EdU assay

The proliferation level of NPC cells under radiation (8 Gy) was determined using EdU assay. More specifically, the EdU Apollo DNA *in vitro* kit was used to perform this experiment and was bought from RIBOBIO (C10341-3, Guangzhou, China). First, 4×10^3 cells/well cells were seeded into 96-well plates with irradiation. After 48 hours of incubation, 3 random fields under a fluorescence microscope were selected, and the EdU positive cells were counted. The EdU positive rate (EdU positive cell number/DAPI positive cell number) represented the proliferation condition of the cells.

Flow cytometric apoptosis assay

Flow cytometry was employed to detect the apoptosis ability of the samples. SUNE-1 and C666-1 cells were

irradiated (8 Gy) and cultured in a 60 mm culture dish for 72 hours before the commencement of the experiments. Briefly, the cells suspended (1×10^5 cells) were inserted into each tube and centrifugalized to lose the culture media. The cells were then washed twice with cold PBS. Next, the cold PBS was removed. After that, 100 µl 1 × binding buffer (Beyotime, China) was added to the cells, and the cells were re-suspended. 5 µl Annexin V (Beyotime, China) and 5 µl PI (Beyotime, China) were diluted with 100 µl 1 × binding buffer, and the solution was then added to the cells in the absence of light. The mixture was subsequently incubated for 15 min. 300 µl 1 × binding buffer was later added to the cells, and the cells were re-suspended again. The cell suspension was then moved to 5 ml flow tubes. After 1 h, flow cytometry analysis was performed on the cells.

Statistical analyses

All the data were analyzed using GraphPad Prism 8.0, and three independent experiments were performed to obtain the results. The data were expressed as mean ± SD (standard deviation). The two-tailed t-test was used to analyze the differences between two groups, whereas the one-way analysis of variance (ANOVA) with Dunnett's post hoc test was used to evaluate the differences between multiple groups. P-values less than 0.05 were regarded as statistically significant.

Results

ENO2 and miR-7-5p were identified as the potential downstream interactome of ZFAS1 in NPC

The WebGestalt algorithm (Figure 1a-b) and Metascape algorithm (Figure 1c-d) were used to enrich the pathway and GO terms of GSE48503 differentially expressed genes (DEGs). The results showed that the glycolytic and HIF-1 pathways were the primary enriched pathways in NPC radioresistance. The glycolytic and HIF-1 pathways were also found to be closely associated with the radioresistance of cancers [45–48]. Previous studies have shown that hypoxia and hypoxia-induced expression of HIF-1 could enhance the resistance of cancer cells to radiotherapy [49,50]. We thus hypothesized that the genes involved in the glycolytic and/or HIF-1 pathways could have a significant impact on NPC radioresistance. Our findings revealed that ENO2 and EGLN3 were the two genes with this potential. Thus, we used the STRING algorithm to further analyze the strength of the interactions between the DEGs. Based on our results, ENO2 showed the most interaction evidence with its neighboring genes (Figure 1e). For this reason, we chose ENO2 as our object of study.

After selecting ENO2, we identified common miRNAs that were both downstream targets of ZFAS1 and upstream regulators of ENO2. The downstream target miRNAs of ZFAS1 were obtained from the ENCORI database (http://starbase.sysu.edu.cn/), and the upstream regulating miRNAs of ENO2 were obtained from TargetScan Human 7.2 (http://targetscan.org/vert_72/). After that, the expression patterns of the overlapped six miRNAs were eventually explored with the dbDEMC database (Figure 1f). Our findings revealed that the six miRNAs were significantly downregulated in NPC cells. Nonetheless, we knew that miR-7-5p was a significant tumor suppressor in many human cancers and that its role in NPC under irradiation has not yet been investigated. To fill this gap, we selected miR-7-5p to be our miRNA of interests.

ZFAS1 was upregulated in NPC cell lines and was located in the cytoplasm

ZFAS1 had a higher expression level in NPC tissues than in adjacent healthy tissues (Figure 2a). Besides, the expression of ZFAS1 was found to be significantly more upregulated in NPC cell lines (SUNE-1, 5–8 F and C666-1) than in normal nasal mucosal epithelial cell NP-69 (Figure 2b). The outcome of our qRT-PCR analysis showed that ZFAS1 was majorly located in the cytoplasm (Figure 2c). Before further experiments were conducted, we confirmed the transfection efficiency of ZFAS1 siRNAs in both cell lines (Figure 2d).

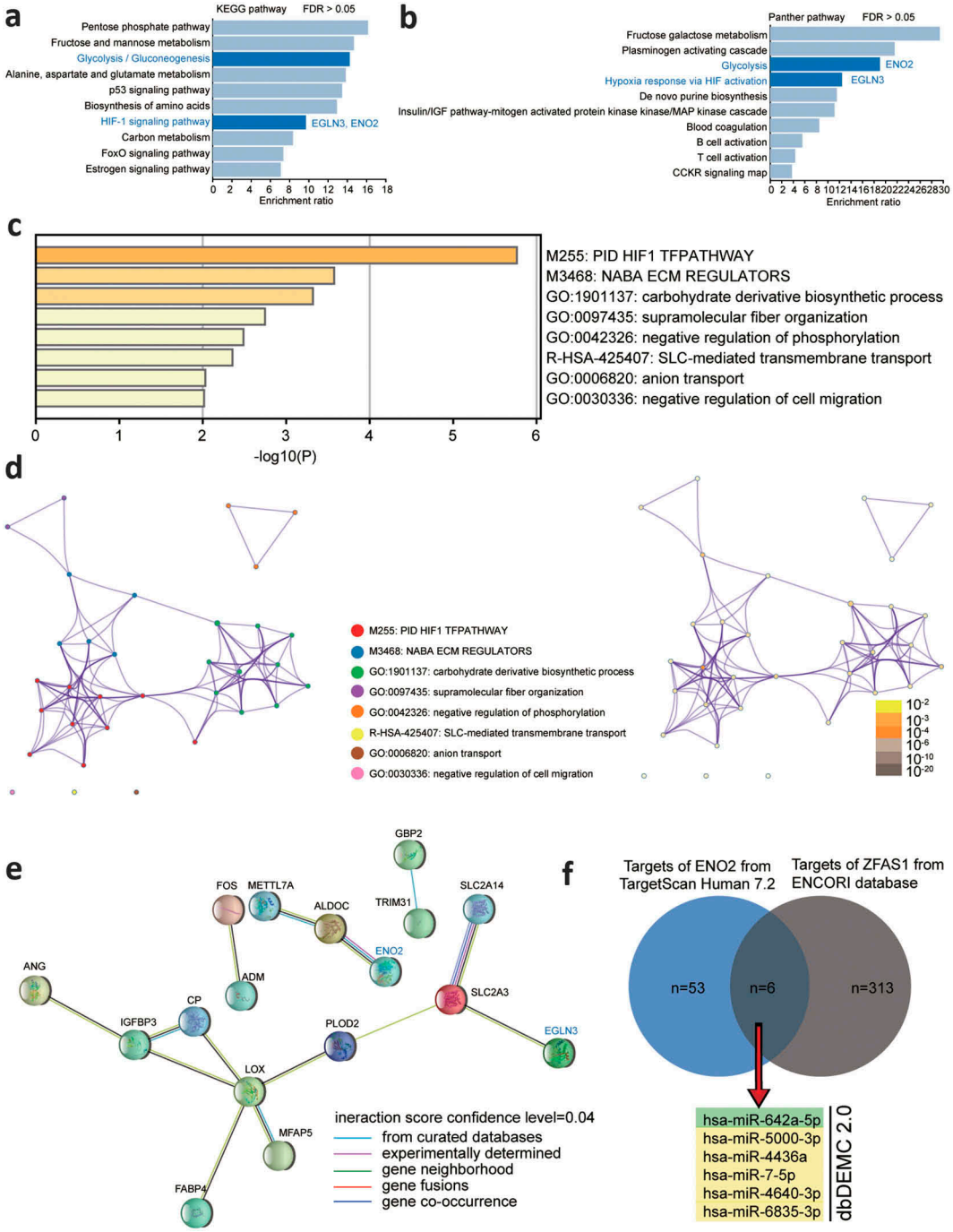

Figure 1. The identification of potential mRNAs and miRNAs that participated in NPC radioresistance.
KEGG pathway enrichment of GSE48503 DEGs using the WebGestalt algorithm (http://www.webgestalt.org/option.php). B. Panther pathway enrichment of GSE48503 DEGs using the WebGestalt algorithm. C. The heatmap of GSE48503 DEGs. D. The enrichment cluster of GSE48503 DEGs. E. STRING analysis revealed the interaction between the DEGs. F. The overlapped miRNAs of the targets of ENO2 were predicted by TargetScan Human 7.2 and those of ZFAS1 were predicted by ENCORI.

ZFAS1 knockdown increased the radiation sensitivity of NPC *in vitro*

To explore whether the knockdown of ZFAS1 could increase the irradiation sensitivity of NPC cells, we detected the survival outcomes of NPC cells under different doses of irradiation treatments and under different timing using CCK-8 assay. Our findings indicated that apart from the increase in irradiation, the knockdown of ZFAS1 decreased cell survival compared with the control group (Figure 3a). We

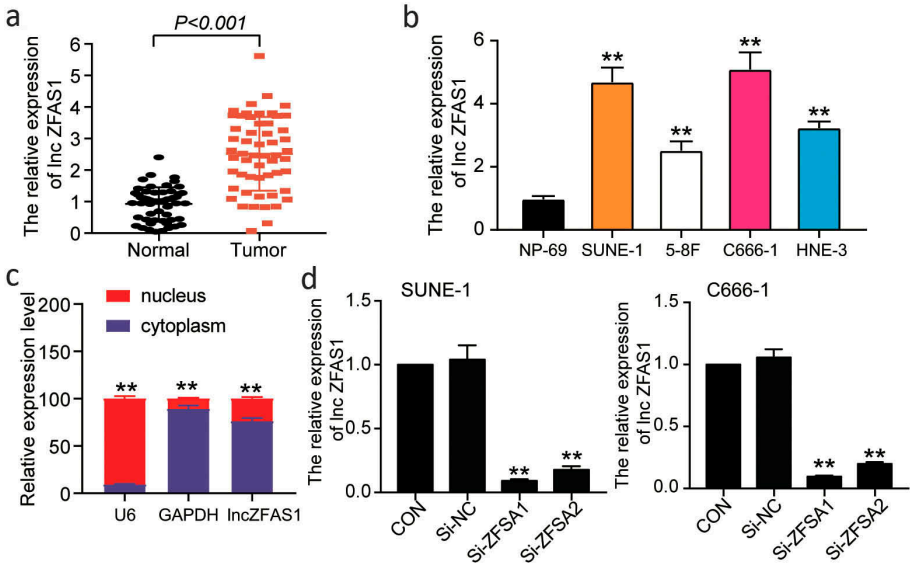

Figure 2. ZFAS1 was upregulated in NPC cells and located in the cytoplasm.

The different expression levels of ZFAS1 between NPC tissues and normal adjacent tissues were measured using qRT-PCR. B. The different expressions of ZFAS1 between NPC cell lines (SUNE-1, 5–8 F, HNE-3and C666-1) and normal nasal mucosal epithelial cell line (NP-69) were detected using qRT-PCR. **P < 0.01, compared with NP-69 cells. C. The expression of ZFAS1 at nuclear or cytoplasm in SUNE-1 and C666-1 cell lines was measured using qRT-PCR. **P < 0.01, compared with the corresponding cytoplasm. D. The transfection efficiency validation of si-ZFAS1-1 and si-ZFAS1-2, which are siRNAs that target ZFAS1 using qRT-PCR. **P < 0.01, compared with the control group.

also found that exposure to 8 Gy irradiation produced the lowest survival rate in SUNE-1 and C666-1 cell lines. In addition, under 8 Gy irradiation treatment, the survival rate of both cell lines significantly decreased in a time-dependent manner (Figure 3b). Next, we observed from the EdU assay results that both si-ZFAS1s decreased the proliferation of SUNE-1 and C666-1 cell lines compared with the control group. The EdU positive rate in ZFAS1 knockdown groups was significantly downregulated in SUNE-1 cell lines (CON 56.76% ±5 vs. SI-ZFAS1 36.67% ±3 and SI-ZFAS2 40.74% ±4) and C666-1 cell lines (CON 63.46% ±6 vs. SI-ZFAS1 46.51% ±4, SI-ZFAS1 45.31% ±4) (Figure 3c). Furthermore, the knockdown of si-ZFAS1 resulted in more apoptotic cells than did the control group under 8 Gy irradiation treatments. We even noticed that the apoptosis rate in ZFAS1 knockdown groups was more than 2-fold compared to the control group (Figure 3d).

ZFAS1: the upstream of miR-7-5p

The binding sequences of ZFAS1 (Figure 4a) on miR-7-5p were obtained from ENCORI. To determine the relationship between ZFAS1 and miR-7-5p, we carried out both luciferase reporter assay and RNA pull-down assay. The result of the luciferase reporter gene assay suggested that compared with other groups, wild type ZFAS1 could bind with miR-7-5p to decrease the fluorescence intensity (Figure 4b). RNA pull-down assay results also showed that ZFAS1 was more enriched with miR-7-5p mimics than with antisense oligo or miR-7-5p mutant (Figure 4c). Moreover, the expression of miR-7-5p was significant lower in NPC tissues than in the adjacent tissues (Figure 4d). After performing an experiment to detect the miR-7-5p expression in NPC cell lines and normal control cell line NP-69, we discovered that miR-7-5p was significantly downregulated in NPC cell lines in contrast to NP-69 (Figure 4e). It was also revealed that ZFAS1 had a negative association with miR-7-5p (figure 4f). It is important to note that before we conducted subsequent experiments, we examined the transfection efficiency of certain molecules. To be precise, after the transfection of si-ZFAS1 (si-ZFAS1-1), miR-892b inhibitor, si-NC and si-ZFAS1 + miR-7-5p inhibitor, we observed that the expression of the si-ZFAS1 group was 1.5-fold more than that of miR-7-5p and that the expression of the miR-7-5p

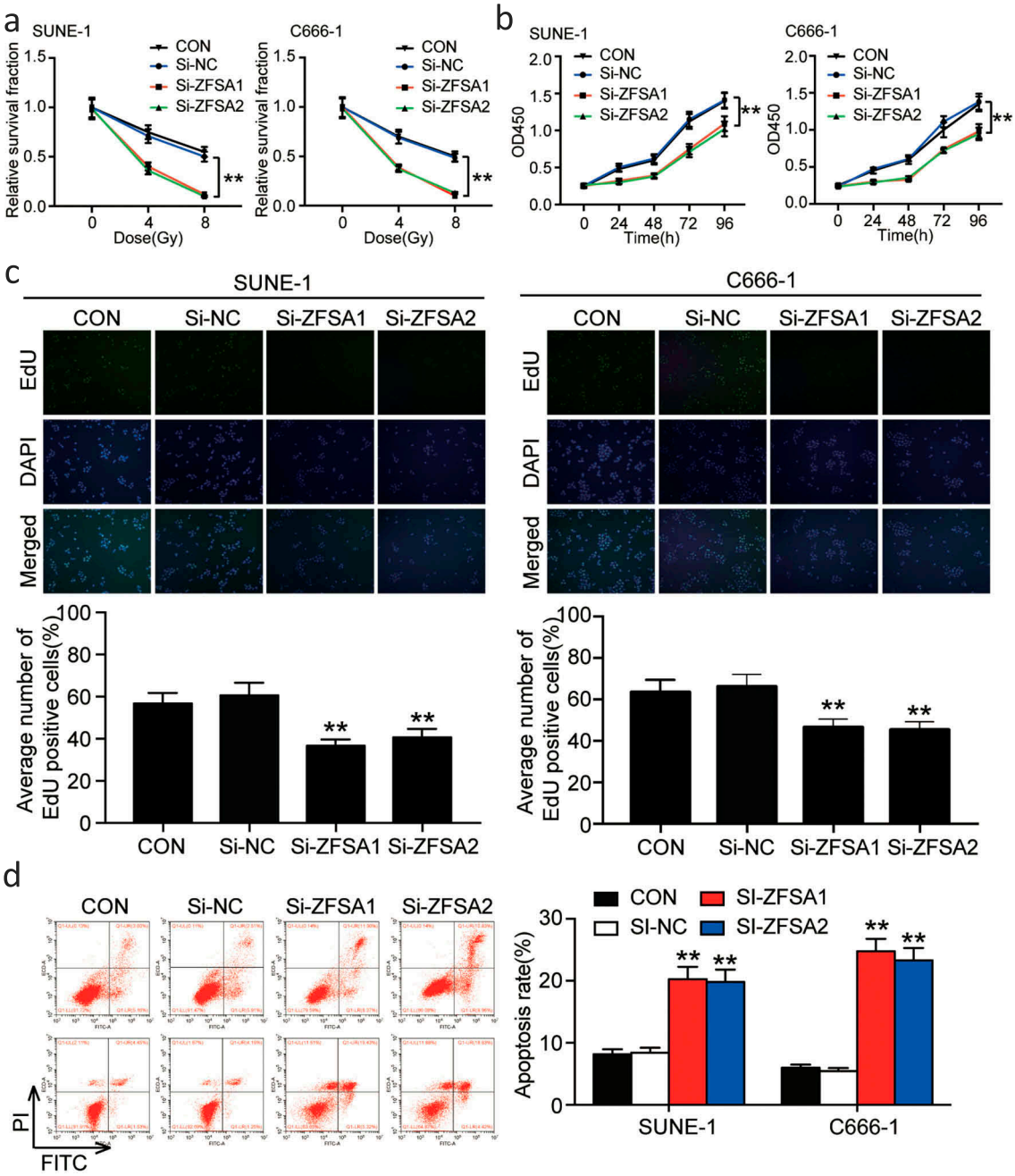

Figure 3. ZFAS1 knockdown weakened the radiation resistance of NPC cells *in vitro*.

The viability changes of NPC cell lines SUNE-1 and C666-1 after providing different doses of irradiation. B. At 8 Gy irradiation, the survival rate of cells in every group was detected at 24, 48, 72, and 96 h in SUNE-1 and C666-1 cell lines. C. Average numbers of EdU positive cells in SUNE-1 and C666-1 cell lines with 8 Gy irradiation. D. The cell apoptosis of SUNE-1 and C666-1 cell lines with 8 Gy irradiation was detected using flow cytometry. **P < 0.01, compared with the control group.

inhibitor group was 75% less than that of miR-7-5p compared with the control group. In addition, the expression of miR-7-5p showed no significant difference between the co-transfection of the si-ZFAS1 and miR-7-5p inhibitor group and the control group (Figure 4g).

ZFAS1 knockdown promoted the radiation sensitivity of NPC cells by acting on miR-7-5p

To further discuss how ZFAS1 impacted on the radiation sensitivity of NPC by regulating miR-7-5p, we designed a rescue experiment. Our CCK-8 assay results suggested that si-ZFAS1 decreased

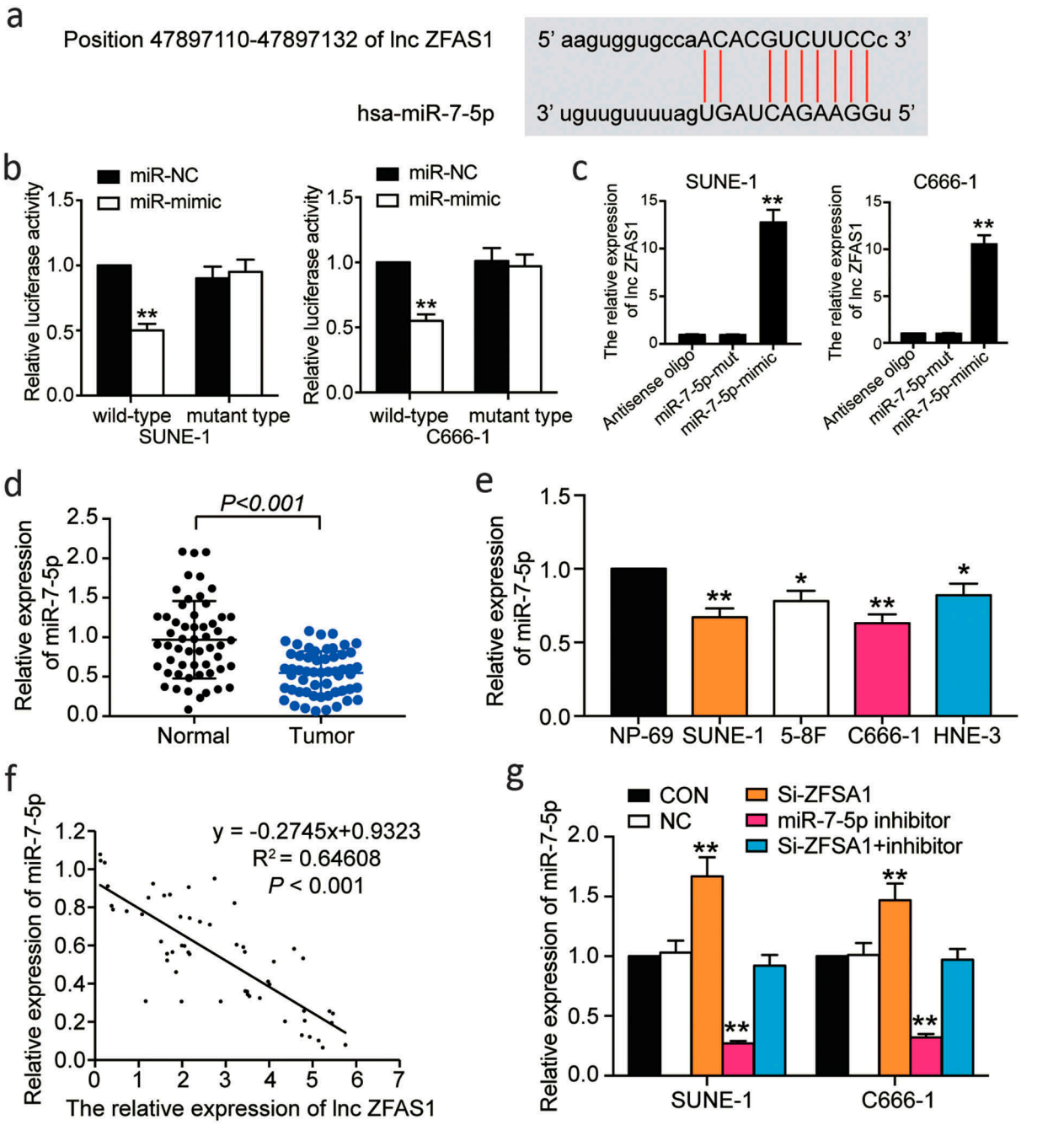

Figure 4. ZFAS1 was the upstream gene of miR-7-5p. A. The predicted binding sequences between ZFAS1 and miR-7-5p were obtained from the ENCORI algorithm.

Luciferase reporter assay was used to determine the target relationship between ZFAS1 and miR-7-5p. **P < 0.01, compared with the miR-NC group. NC: negative control. C. RNA pull-down assay was performed to demonstrate the association between ZFAS1 and miR-7-5p. mut: mutant. **P < 0.01, compared with the antisense oligo group. D. The expression of miR-7-5p in NPC tissues and adjacent tissues. E. The expression of miR-7-5p in NPC cell lines. *P < 0.05, **P < 0.01, compared with NP-69 cell line. F. ZFAS1 expression showed a negative relationship with miR-7-5p expression. G. The transfection efficiency of miR-7-5p inhibitor. **P < 0.01, compared with the control group.

the viability of SUNE-1 cells at 48 h, 72 h and 96 h, as well the viability of C666-1 cells at 72 h and 96 h. This decrease was offset by the introduction of miR-7-5p inhibitor in an environment of 8 Gy irradiation (Figure 5a). Also, the result of the EdU assay was similar to that of the CCK-8 assay. While the proliferation ability of SUNE-1 and C666-1 cells significantly decreased in the si-ZFAS1 group, it

increased in the miR-7-5p inhibitor group. We noticed that the EdU positive rate in the si-ZFAS1 group dropped by 50% in SUNE-1 cells and 25% in C666-1 cells, but it increased by 20% in the miR-7-5p inhibitor group. After co-transfecting miR-7-5p inhibitor and si-ZFAS1 into NPC samples, we found that the proliferating cells increased in contrast to the si-ZFAS1 group (Figure 5b). Besides, we found that si-ZFAS1 promoted cell apoptosis, while miR-7-5p inhibitor inhibited cell apoptosis in SUNE-1 and C666-1 cell lines. The apoptosis rate in the si-ZFAS1 group was more than 2-fold of that of the control group, whereas the apoptosis rate in the miR-7-5p inhibitor group was merely less than half of that of the control group. The apoptotic cells were finally recovered after the transfection of miR-7-5p inhibitor and si-ZFAS1 (Figure 5c).

MiR-7-5p was the upstream target gene of ENO2 mRNA

Figure 6a illustrates the binding scheme predicted by TargetScan Human 7.2 (http://www.targetscan.org/vert_72/) and shows the targeting relationship between miR-7-5p and ENO2 mRNA. The binding relationship was validated using dual-luciferase reporter gene assay and RNA pull-down assay. The outcome of the luciferase reporter assay demonstrated that wide-type ENO2 mRNA could be targeted by miR-7-5p and decrease fluorescence intensity compared with other groups (Figure 6b). RNA pull-down assay results showed that ENO2 was significantly enriched with the addition of miR-7-5p mimics contrast to antisense oligo and miR-7-5p mutant groups in both SUNE-1 cell line and C666-1 cell line (Figure 6c). After carrying out qRT-PCR to detect ENO2 mRNA expression in NPC tissues and NPC cell lines, we found that ENO2 mRNA was significantly upregulated in NPC tissues and cells (Figure 6d-e). The expression of miR-7-5p and ENO2 mRNA was negatively associated (Figure 6f). In addition, we built cell models stably transfected with si-NC, si-ENO2, miR-7-5p inhibitor, and si-ENO2+ miR-7-5p inhibitor for further experiments (Figure 6g).

MiR-7-5p inhibition enhanced the radiation resistance of NPC cells by acting on ENO2 mRNA

To further explore the role of miR-7-5p in influencing the radioresistance of NPC cells by regulating ENO2 mRNA, we performed rescue experiments. The results of the CCK-8 assay suggested that in an environment with 8 Gy irradiation, si-ENO2 significantly weakened the cell viability of NPC cells with the miR-7-5p inhibitor offsetting the effect at 72 h and 96 h in both SUNE-1 and C666-1 cell lines (Figure 7a). The EdU assay also demonstrated a similar result with the CCK-8 assay: Cell proliferation in SUNE-1 and C666-1 cell lines decreased in the si-ENO2 group but increased in the miR-7-5p inhibitor group. Furthermore, after the miR-7-5p inhibitor was co-transfected with si-ENO2, we found that the proliferation ability of the cells increased compared to the si-ENO2 group (Figure 7b). Besides, we found that si-ENO2 promoted cell apoptosis by almost 50%, while miR-7-5p inhibitor inhibited cell apoptosis by almost 50% in SUNE-1 and C666-1 cell lines. The cell apoptosis increased when miR-7-5p inhibitor and si-ENO2 were co-transfected compared with the si-ENO2 group (Figure 7c). Figure 8 illustrates the hypothesized mechanism in NPC radioresistance involving ZFAS1, miR-7-5p and ENO2. High ZFAS1 and ENO2 levels with low miR-7-5p level resulted in more resistance to the irradiation of cancerous cells. For instance, ZFAS1 promoted NPC cell's resistance to irradiation by downregulating miR-7-5p, thereby releasing more ENO2 mRNA.

Discussion

We observed in this research that ZFAS1 was significantly upregulated in NPC tissues and ENO2, while miR-7-5p was downregulated in NPC tissues. Our results also revealed that ZFAS1 knockdown weakened radioresistance of NPC *in vitro*. We also found that ZFAS1 could sponge miR-7-5p and regulate ENO2 targeted by miR-7-5p. To further explore how ZFAS1 affected irradiation sensitivity, we transfected miR-7-5p inhibitor and ENO2 siRNA to SUNE-1 and C666-1 cell lines with irradiation. Overall, we discovered that ZFAS1 enhanced the

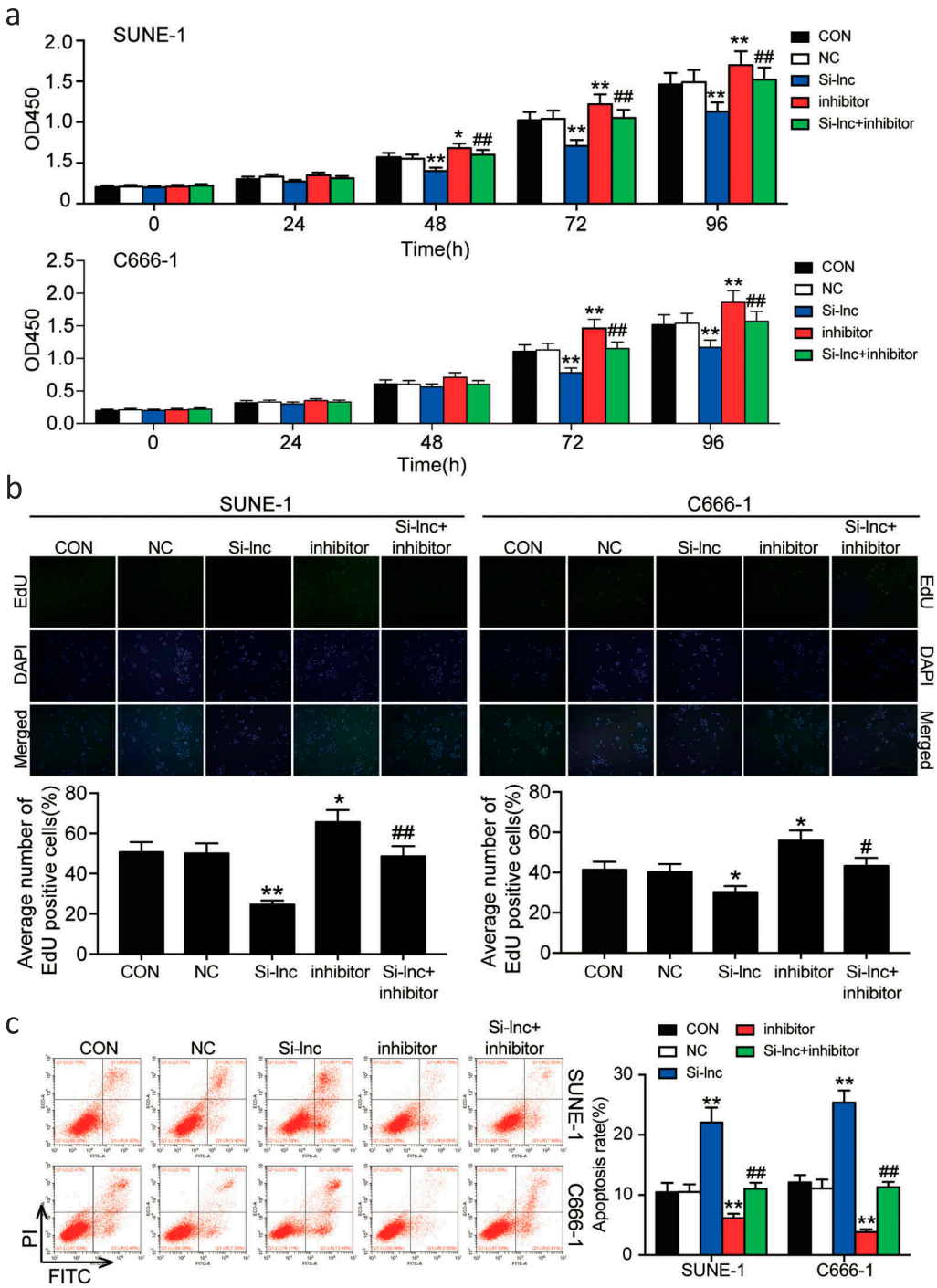

Figure 5. The knockdown of ZFAS1 suppressed the radiation resistance of NPC cells by acting on miR-7-5p.

CCK-8 assay was used to detect the viability of SUNE-1 and C666-1 cells after transfecting with si-ZFAS1 or miR-7-5p inhibitor under 8 Gy irradiation. B. EdU assay was used to observe the cell proliferation of SUNE-1 and C666-1 cell lines after transfecting with si-ZFAS1 or miR-7-5p under 8 Gy irradiation. C. The cell apoptosis in SUNE-1 and C666-1 cell lines after transfecting with si-ZFAS1 or miR-7-5p inhibitor with giving 8 Gy irradiation by flow cytometry. *P < 0.05, **P < 0.01, compared with the control group; #P < 0.05, ##P < 0.01, compared with the miR-7-5p inhibitor group.

radioresistance of NPC cells by sponging miR-7-5p to upregulate ENO2.

Radiotherapy is currently the main treatment for patients with NPC. However, because of the radioresistance of NPC cells, the five-year survival rate of NPC patients treated with radiotherapy is still not ideal [51]. Some recent studies revealed that the expression of some lncRNAs affected the radiation

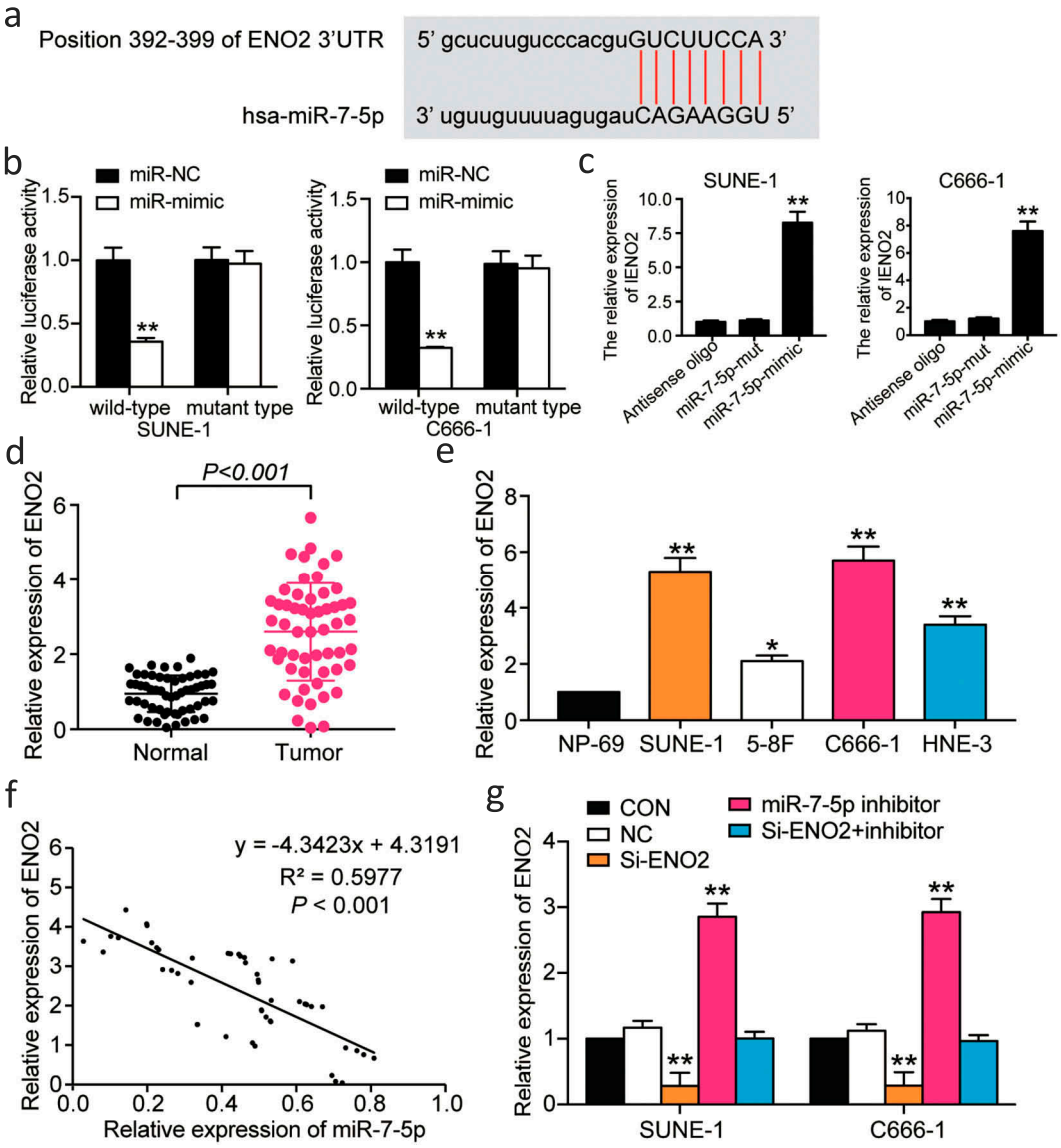

Figure 6. MiR-7-5p was the upstream target gene of ENO2.

The illustration of the predicted binding sites of miR-7-5p and ENO2 mRNA. B. Luciferase reporter assay results showed that ENO2 was the downstream target gene of miR-7-5p. **P < 0.01, compared with the miR-NC group C. The RNA pull-down assay results demonstrated the regulatory relationship between ENO2 and miR-7-5p. **P < 0.01, compared with the antisense oligo group. D. The expression of ENO2 mRNA in NPC tissues and adjacent healthy tissues. E. The expression of ENO2 in NPC cell lines and normal cell NP-69. *P < 0.05, **P < 0.01, compared with NP-69 cell line. F. ENO2 mRNA expression had a negative relationship with miR-7-5p expression. G. qRT-PCR was used to observe the expression of ENO2 mRNA in SUNE-1 and C666-1 cells after transfecting with si-ZFAS1 or miR-7-5p. **P < 0.01, compared with the control group.

resistance of NPC. For instance, higher levels of lncRNA ANCR promoted the cell proliferation and radiation resistance of NPC samples [52]. The expression of lncRNA MINCR also promoted the radiation resistance of NPC cells by regulating the miR-223/ZEB1 axis [5]. Many studies confirmed that the expression of ZFAS1 was related to the drug resistance of multiple types of tumors. For instance, a study reported that the expression of ZFAS1 could enhance the drug resistance of acute lymphoblastic leukemia to Adriamycin [53]. In the last two years, lncRNA ZFAS1 has been discovered to promote the development of NPC by activating the Wnt/β-actin pathway [54] and inhibiting the PI3K/AKT pathway [55]. In our previous study, lncRNA ZFAS1 was also found to be highly expressed in NPC tissues and to augment NPC by regulating miR-893b-LPAR1 interactome [20].

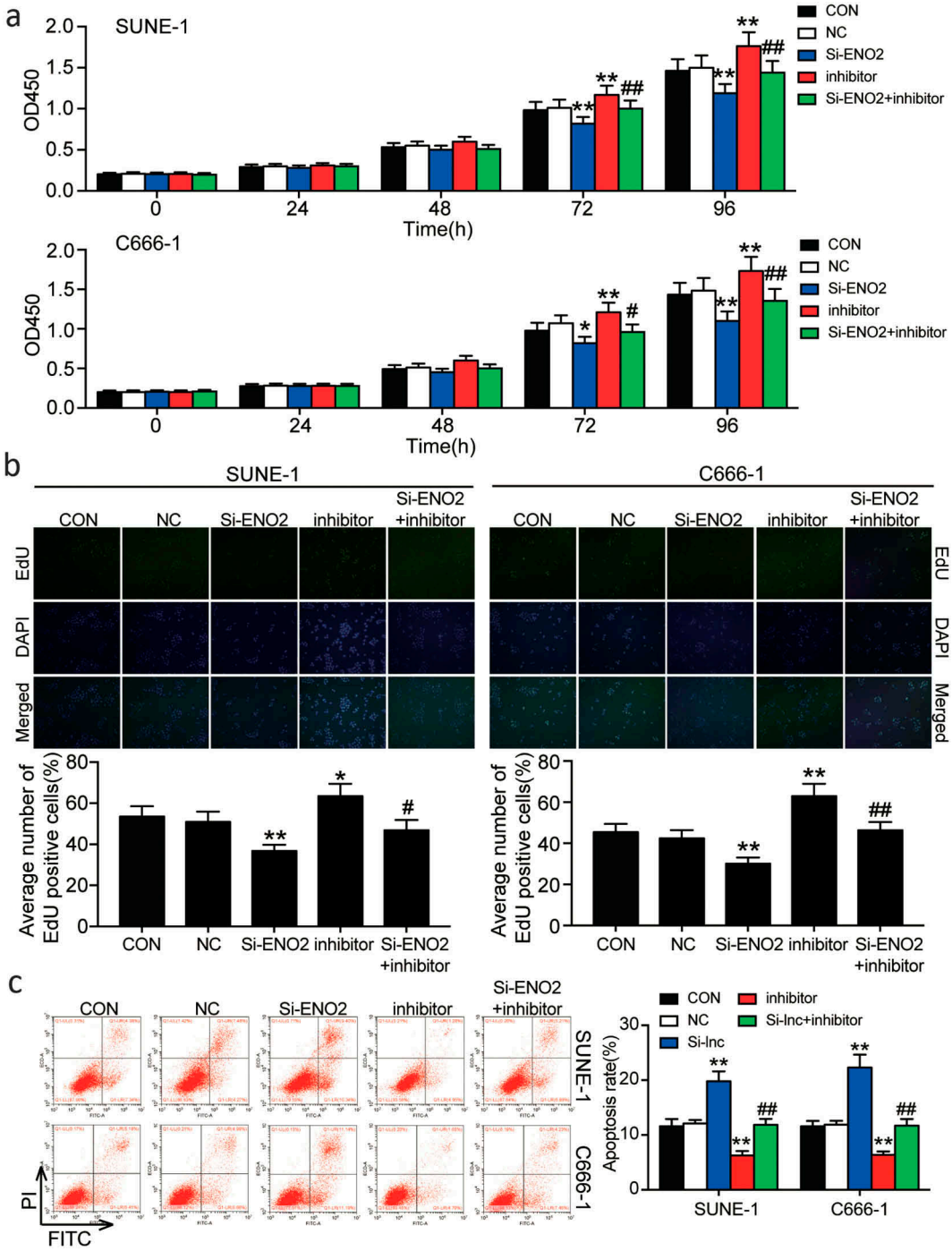

Figure 7. MiR-7-5p inhibition enhanced the radiation resistance of NPC cells by acting on ENO2.

CCK-8 assay results showed that si- ENO2 suppressed the cell viability of SUNE-1 and C666-1 cell lines, while miR-7-5p inhibition promoted the cell viability at 8 Gy irradiation. B. EdU assay results indicated that si-ENO2 suppressed the growth of SUNE-1 and C666-1 cell lines, while miR-7-5p inhibition enhanced the cell viability at 8 Gy irradiation. C. The cell apoptosis in SUNE-1 and C666-1 cell lines after transfecting with si-ENO2 and miR-7-5p inhibitor under 8 Gy irradiation. *P < 0.05, **P < 0.01, compared with the control group; #P < 0.05, ##P < 0.01, compared with the miR-7-5p inhibitor group.

However, whether ZFAS1 could affect the radiation resistance of NPC is unclear. We speculated that the expression of ZFAS1 could enhance the radioresistance of NPC. After performing a cytological experiment, we observed that knocking down lncRNA ZFAS1 inhibited the proliferation, migration and invasion of NPC cells but that it induced the apoptosis of NPC cells with irradiation treatment.

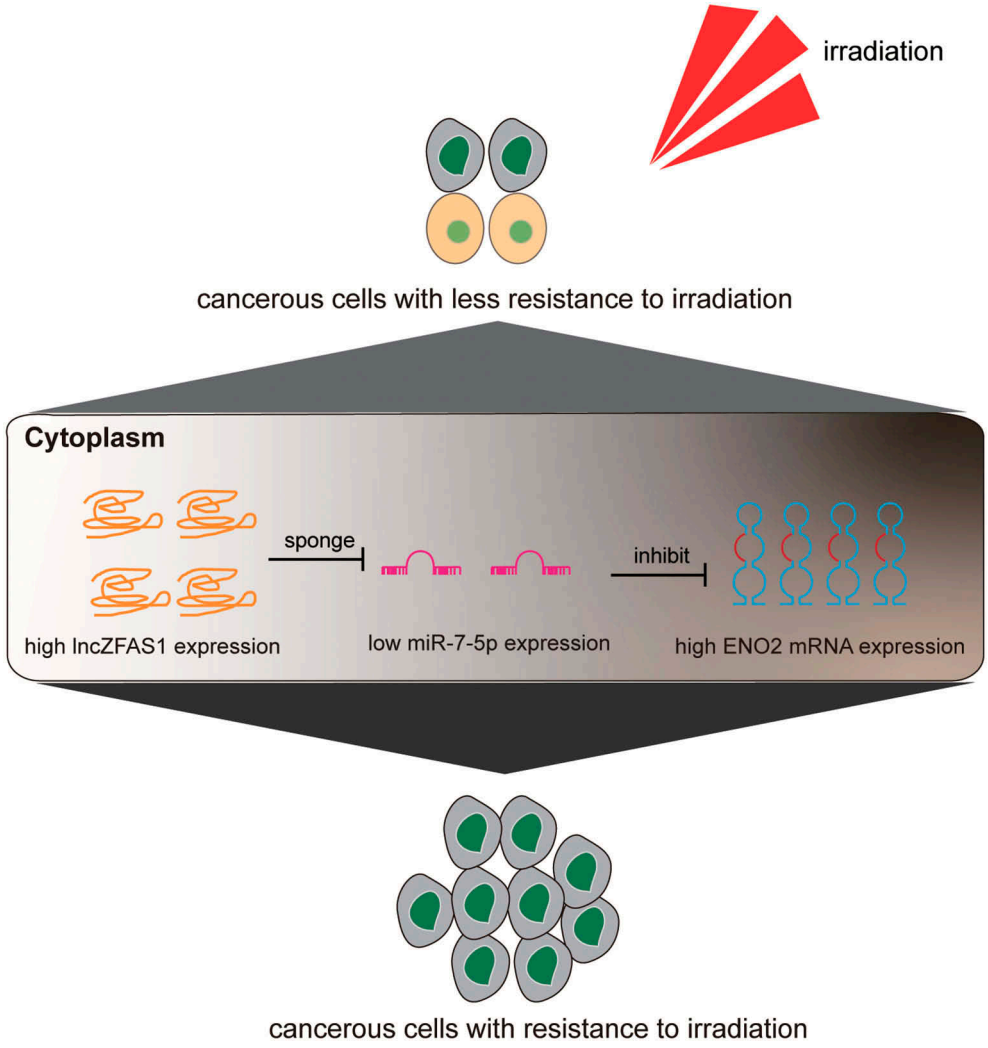

Figure 8. The illustration of the hypothesized mechanism involving ZFAS1, miR-7-5p and ENO2 in NPC radioresistance. Basically, high ZFAS1 level, low miR-7-5p level, and high ENO2 mRNA level in NPC results enhanced radioresistance.

Furthermore, we performed a bioinformatics analysis and found that lncRNA ZFAS1 could sponge and restrict the biological effects of miR-7-5p. In the last 10 years, miR-7-5p has been discovered to be a tumor suppressor in various human cancers. It was found to play a tumor-suppressing role in gastric cancer [56] and colorectal cancer [57]. In a study that involved patients with NPC, miR-7-5p was found to suppress colony formation significantly [58]. As for radiation resistance, one research revealed that miR-7-5p with a high level of expression could promote the radiation resistance of cervical cancer and hepatoma cancer cells after being radiated (5 Gy and 10 Gy) [28]. However, we found that the miR-7-5p inhibitor significantly enhanced the radioresistance of NPC cells by promoting cell proliferation, migration and invasion and suppressing cell apoptosis. Moreover, miR-7-5p, a downstream of ZFAS1, could counteract the promotive effect of ZFAS1 on radioresistant NPC cells.

Changes in metabolic patterns are associated with the development of cancer. This study found that the glycolytic and HIF-1 pathways were closely related to the radioresistance of NPC. According to the results of previous studies, the glycolytic and HIF-1 pathways were associated with the radioresistance of cancers [45–48]. Hence, we identified key gene ENO2 involved in glycolysis and the HIF-1 pathway using the STRING algorithm. It was reported that ENO2 could affect the proliferation of breast cancer cells [59]. ENO2 was also documented to be involved in the glycolytic pathway in renal cell carcinoma [44] and colorectal cancer [60]. As for chemotherapy

resistance, ENO2 contributed to the chemotherapy resistance of leukemia cells by promoting the progress of glycolysis [43]. After combining the results of bioinformatics analysis and previous studies, we predicted that ENO2 might influence the radioresistance of NPC.

In this study, we proved that the expression of ENO2 was upregulated in NPC. We also showed that the inhibition of ENO2 could repress the malignancy of NPC cells with irradiation. Besides, our results revealed that ENO2 could be targeted by miR-7-5p in NPC. This means that this gene could regulate the inhibitory effect of miR-7-5p on radioresistant NPC cells. Also identified in this research was that ENO2 could shape the hypoxia response by regulating the HIF-1 signaling. Previous studies have shown that hypoxia could promote the radiation-resistant of tumor cells [61,62]. Even though HIF-1 signaling has been regarded as crucial signaling in the radioresistance of human cancers [63], we are yet to study the role of ZFAS1 on tumor hypoxia and research how ENO2 regulated the HIF-1α pathway. In addition, experiments on animals are yet to be conducted to validate the effects of the interactome *in vivo*. In conclusion, our experiment suggested that lncRNA ZFAS1 acted as a radiation-resistance enhancer in NPC. ZFAS1 could competitively bound with miR-892b, thereby increasing the expression of ENO2 to enhance the radiation resistance of NPC cells.

Disclosure of interest

The authors declare that no conflict of interests exists in this research.

Disclosure statement

No potential conflict of interest was reported by the authors.

Data availability statement

The datasets used and analyzed during the current study are available from the corresponding author on reasonable request.

Ethics approval and consent to participate

The study was approved by the ethic committee of West China Hospital, Sichuan University. Written informed consent was obtained from all participates.

Authors' contributions

JJP, FL, HZ, QW made substantial contributions to the experimental design; JJP, FL, HZ, QW, SXL contributed to acquisition, analysis and interpretation of data; JJP, FL, SXL drafted the manuscript; SXL revised the paper and provided feedback; All authors read and approved the final manuscript.

References

[1] Lu Y, Liang Y, Zheng X, et al. EVI1 promotes epithelial-to-mesenchymal transition, cancer stem cell features and chemo-/radioresistance in nasopharyngeal carcinoma. J Exp Clin Cancer Res. 2019;38(1):82.

[2] Guo Y, Zhai J, Zhang J, et al. Improved radiotherapy sensitivity of nasopharyngeal carcinoma cells by miR-29-3p targeting COL1A1 3⊠-UTR. Med Sci Monit. 2019;25:3161–3169.

[3] Gupta AK, McKenna WG, Weber CN, et al. Local recurrence in head and neck cancer: relationship to radiation resistance and signal transduction. Clin Cancer Res. 2002;8(3):885–892.

[4] Hildesheim A, Wang CP. Genetic predisposition factors and nasopharyngeal carcinoma risk: a review of epidemiological association studies, 2000-2011: rosetta stone for NPC: genetics, viral infection, and other environmental factors. Semin Cancer Biol. 2012;22(2):107–116.

[5] Zhong Q, Chen Y, Chen Z. LncRNA MINCR regulates irradiation resistance in nasopharyngeal carcinoma cells via the microRNA-223/ZEB1 axis. Cell Cycle. 2020;19(1):53–66.

[6] Liang ZG, Lin GX, Yu BB, et al. The role of autophagy in the radiosensitivity of the radioresistant human nasopharyngeal carcinoma cell line CNE-2R. Cancer Manag Res. 2018;10:4125–4134.

[7] Lee AW, Ma BB, Ng WT, et al. Management of nasopharyngeal carcinoma: current practice and future perspective. J Clin Oncol. 2015;33(29):3356–3364.

[8] Kong F, Ying H, Du C, et al. Patterns of local-regional failure after primary intensity modulated radiotherapy for nasopharyngeal carcinoma. Radiat Oncol. 2014;9:60.

[9] Sun W, Wu Y, Yu X, et al. Decreased expression of long noncoding RNA AC096655.1-002 in gastric cancer and its clinical significance. Tumour Biol. 2013;34(5):2697–2701.

[10] Engreitz JM, Pandya-Jones A, McDonel P, et al. The Xist lncRNA exploits three-dimensional genome architecture to spread across the X chromosome. Science. 2013;341(6147):1237973.

[11] Ard R, Tong P, Allshire RC. Long non-coding RNA-mediated transcriptional interference of a permease gene confers drug tolerance in fission yeast. Nat Commun. 2014;5:5576.

[12] Kanduri C. Long noncoding RNAs: lessons from genomic imprinting. Biochim Biophys Acta. 2016;1859(1):102–111.
[13] Li Y, Wang Z, Shi H, et al. HBXIP and LSD1 scaffolded by lncRNA hotair mediate transcriptional activation by c-Myc. Cancer Res. 2016;76(2):293–304.
[14] Sun M, Nie F, Wang Y, et al. LncRNA HOXA11-AS promotes proliferation and invasion of gastric cancer by scaffolding the chromatin modification factors PRC2, LSD1, and DNMT1. Cancer Res. 2016;76(21):6299–6310.
[15] Askarian-Amiri ME, Crawford J, French JD, et al. SNORD-host RNA Zfas1 is a regulator of mammary development and a potential marker for breast cancer. RNA. 2011;17(5):878–891.
[16] Li T, Xie J, Shen C, et al. Amplification of long noncoding RNA ZFAS1 promotes metastasis in hepatocellular carcinoma. Cancer Res. 2015;75(15):3181–3191.
[17] Cui X, Piao C, Lv C, et al. ZNFX1 anti-sense RNA 1 promotes the tumorigenesis of prostate cancer by regulating c-Myc expression via a regulatory network of competing endogenous RNAs. Cell Mol Life Sci. 2020;77(6):1135–1152.
[18] Xia L, Wu L, Bao J, et al. Circular RNA circ-CBFB promotes proliferation and inhibits apoptosis in chronic lymphocytic leukemia through regulating miR-607/FZD3/Wnt/beta-catenin pathway. Biochem Biophys Res Commun. 2018;503(1):385–390.
[19] Li Z, Qin X, Bian W, et al. Exosomal lncRNA ZFAS1 regulates esophageal squamous cell carcinoma cell proliferation, invasion, migration and apoptosis via microRNA-124/STAT3 axis. J Exp Clin Cancer Res. 2019;38(1):477.
[20] Peng J, Liu F, Zheng H, et al. Long noncoding RNA ZFAS1 promotes tumorigenesis and metastasis in nasopharyngeal carcinoma by sponging miR-892b to up-regulate LPAR1 expression. J Cell Mol Med. 2020;24(2):1437–1450.
[21] Ko J, Bhagwat N, Black T, et al. miRNA profiling of magnetic nanopore-isolated extracellular vesicles for the diagnosis of pancreatic cancer. Cancer Res. 2018;78(13):3688–3697.
[22] Telonis AG, Rigoutsos I. Race disparities in the contribution of miRNA isoforms and tRNA-derived fragments to triple-negative breast cancer. Cancer Res. 2018;78(5):1140–1154.
[23] Nagesh PKB, Chowdhury P, Hatami E, et al. miRNA-205 nanoformulation sensitizes prostate cancer cells to chemotherapy. Cancers (Basel). 2018;10:9.
[24] Marcuello M, Duran-Sanchon S, Moreno L, et al. Analysis of A 6-mirna signature in serum from colorectal cancer screening participants as non-invasive biomarkers for advanced adenoma and colorectal cancer detection. Cancers (Basel). 2019;11(10):1542.
[25] Yu L, Wu D, Gao H, et al. Clinical utility of a STAT3-regulated miRNA-200 family signature with prognostic potential in early gastric cancer. Clin Cancer Res. 2018;24(6):1459–1472.
[26] Galka-Marciniak P, Urbanek-Trzeciak MO, Nawrocka PM, et al. Somatic mutations in miRNA genes in lung cancer-potential functional consequences of non-coding sequence variants. Cancers (Basel). 2019;11:6.
[27] Kanlikilicer P, Bayraktar R, Denizli M, et al. Exosomal miRNA confers chemo resistance via targeting Cav1/p-gp/M2-type macrophage axis in ovarian cancer. EBioMedicine. 2018;38:100–112.
[28] Tomita K, Fukumoto M, Itoh K, et al. MiR-7-5p is a key factor that controls radioresistance via intracellular Fe(2+) content in clinically relevant radioresistant cells. Biochem Biophys Res Commun. 2019;518(4):712–718.
[29] Kabir TD, Ganda C, Brown RM, et al. A microRNA-7/growth arrest specific 6/TYRO3 axis regulates the growth and invasiveness of sorafenib-resistant cells in human hepatocellular carcinoma. Hepatology. 2018;67(1):216–231.
[30] Yang F, Guo L, Cao Y, et al. MicroRNA-7-5p promotes cisplatin resistance of cervical cancer cells and modulation of cellular energy homeostasis by regulating the expression of the PARP-1 and BCL2 genes. Med Sci Monit. 2018;24:6506–6516.
[31] Gao D, Zhang X, Liu B, et al. Screening circular RNA related to chemotherapeutic resistance in breast cancer. Epigenomics. 2017;9(9):1175–1188.
[32] Lai J, Yang H, Zhu Y, et al. MiR-7-5p-mediated downregulation of PARP1 impacts DNA homologous recombination repair and resistance to doxorubicin in small cell lung cancer. BMC Cancer. 2019;19(1):602.
[33] Law ML, Kao FT. Regional mapping of the gene coding for enolase-2 on human chromosome 12. J Cell Sci. 1982;53:245–254.
[34] Muller FL, Colla S, Aquilanti E, et al. Passenger deletions generate therapeutic vulnerabilities in cancer. Nature. 2012;488(7411):337–342.
[35] Kim J, Jin H, Zhao JC, et al. FOXA1 inhibits prostate cancer neuroendocrine differentiation. Oncogene. 2017;36(28):4072–4080.
[36] Teng PN, Hood BL, Sun M, et al. Differential proteomic analysis of renal cell carcinoma tissue interstitial fluid. J Proteome Res. 2011;10(3):1333–1342.
[37] Ward PS, Thompson CB. Metabolic reprogramming: a cancer hallmark even warburg did not anticipate. Cancer Cell. 2012;21(3):297–308.
[38] Cassim S, Pouyssegur J. Tumor microenvironment: a metabolic player that shapes the immune response. Int J Mol Sci. 2019;21:1.
[39] Pavlides S, Whitaker-Menezes D, Castello-Cros R, et al. The reverse Warburg effect: aerobic glycolysis in cancer associated fibroblasts and the tumor stroma. Cell Cycle. 2009;8(23):3984–4001.
[40] Vander Heiden MG, Cantley LC, Thompson CB. Understanding the Warburg effect: the metabolic

requirements of cell proliferation. Science. 2009;324 (5930):1029–1033.
[41] Cassim S, Raymond VA, Lacoste B, et al. Metabolite profiling identifies a signature of tumorigenicity in hepatocellular carcinoma. Oncotarget. 2018;9(42):26868–26883.
[42] Cassim S, Raymond VA, Dehbidi-Assadzadeh L, et al. Metabolic reprogramming enables hepatocarcinoma cells to efficiently adapt and survive to a nutrient-restricted microenvironment. Cell Cycle (Georgetown, TX). 2018;17(7):903–916.
[43] Liu CC, Wang H, Wang WD, et al. ENO2 promotes cell proliferation, glycolysis, and glucocorticoid-resistance in acute lymphoblastic leukemia. Cell Physiol Biochem. 2018;46(4):1525–1535.
[44] Zhang T, Niu X, Liao L, et al. The contributions of HIF-target genes to tumor growth in RCC. PLoS One. 2013;8(11):e80544.
[45] Augoff K, Hryniewicz-Jankowska A, Tabola R. Lactate dehydrogenase 5: an old friend and a new hope in the war on cancer. Cancer Lett. 2015;358(1):1–7.
[46] Moreno-Sanchez R, Rodriguez-Enriquez S, Marin-Hernandez A, et al. Energy metabolism in tumor cells. Febs J. 2007;274(6):1393–1418.
[47] Bhattarai D, Xu X, Lee K. Hypoxia-inducible factor-1 (HIF-1) inhibitors from the last decade (2007 to 2016): A "structure-activity relationship" perspective. Med Res Rev. 2018;38(4):1404–1442.
[48] Wigerup C, Pahlman S, Bexell D. Therapeutic targeting of hypoxia and hypoxia-inducible factors in cancer. Pharmacol Ther. 2016;164:152–169.
[49] Semenza GL. Intratumoral hypoxia, radiation resistance, and HIF-1. Cancer Cell. 2004;5(5):405–406.
[50] Semenza GL. Defining the role of hypoxia-inducible factor 1 in cancer biology and therapeutics. Oncogene. 2010;29(5):625–634.
[51] Chua MLK, Wee JTS, Hui EP, et al. Nasopharyngeal carcinoma. Lancet. 2016;387(10022):1012–1024.
[52] Ma X, Zhou J, Liu J, et al. LncRNA ANCR promotes proliferation and radiation resistance of nasopharyngeal carcinoma by inhibiting PTEN expression. Onco Targets Ther. 2018;11:8399–8408.
[53] Liu Q, Ma H, Sun X, et al. The regulatory ZFAS1/miR-150/ST6GAL1 crosstalk modulates sialylation of EGFR via PI3K/Akt pathway in T-cell acute lymphoblastic leukemia. J Exp Clin Cancer Res. 2019;38(1):199.
[54] Chen X, Li J, Li CL, et al. Long non-coding RNA ZFAS1 promotes nasopharyngeal carcinoma through activation of Wnt/beta-catenin pathway. Eur Rev Med Pharmacol Sci. 2018;22(11):3423–3429.
[55] Wang X, Jin Q, Wang X, et al. LncRNA ZFAS1 promotes proliferation and migration and inhibits apoptosis in nasopharyngeal carcinoma via the PI3K/AKT pathway in vitro. Cancer Biomark. 2019;26(2):171–182.
[56] Xin L, Liu L, Liu C, et al. DNA-methylation-mediated silencing of miR-7-5p promotes gastric cancer stem cell invasion via increasing Smo and Hes1. J Cell Physiol. 2020;235(3):2643–2654.
[57] Zheng Y, Nie P, Xu S. Long noncoding RNA CASC21 exerts an oncogenic role in colorectal cancer through regulating miR-7-5p/YAP1 axis. Biomed Pharmacother. 2020;121:109628.
[58] Zhong Q, Huang J, Wei J, et al. Circular RNA CDR1as sponges miR-7-5p to enhance E2F3 stability and promote the growth of nasopharyngeal carcinoma. Cancer Cell Int. 2019;19:252.
[59] Kim BG, Sung JS, Jang Y, et al. Compression-induced expression of glycolysis genes in CAFs correlates with EMT and angiogenesis gene expression in breast cancer. Commun Biol. 2019;2:313.
[60] Yeh CS, Wang JY, Chung FY, et al. Significance of the glycolytic pathway and glycolysis related-genes in tumorigenesis of human colorectal cancers. Oncol Rep. 2008;19(1):81–91.
[61] Schito L, Semenza GL. Hypoxia-inducible factors: master regulators of cancer progression. Trends Cancer. 2016;2(12):758–770.
[62] Yue X, Lan F, Xia T. Hypoxic glioma cell-secreted exosomal miR-301a activates Wnt/β-catenin signaling and promotes radiation resistance by targeting TCEAL7. Mol Ther. 1939-1949;2019(27):11.
[63] Moeller BJ, Dewhirst MW. HIF-1 and tumour radiosensitivity. Br J Cancer. 2006;95(1):1–5.